FACTA UNIVERSITATIS
Series: **Mechanical Engineering** Vol.1, N° 9, 2002, pp. 1231 - 1239

COMPUTER SIMULATION OF CUMULATIVE FATIGUE DAMAGE

UDC 620.152.2/.4=861

Zoran Perović

Faculty of Mechanical Engineering, University of Montenegro
Cetinjski put bb, 81000 Podgorica, E-mail:zoranp@cg.ac.yu

Abstract. *Computer simulation of cumulative fatigue damage of welded joint subjected to variable-amplitude loading is presented in this paper. The crack growth rate for a given material is expressed as a function of an effective range of stress intensity factor in order to account for both short and long crack behaviour. The correction factors in the equation of stress intensity factor were determined by Gross' and Albrecht's methods. The fatigue life is calculated by solving the equation of fatigue crack growth rate from a_0 to a_f by Runge-Kutta method. A computer program, based on this procedure, is used for the fatigue crack growth simulation. The obtained results were compared with the fatigue life determined by using Miner's rule, determining the error of the latter in the region near the variable-amplitude fatigue limit.*

Key words: *cumulative fatigue damage, computer simulation, short and long crack, local plastic zone*

INTRODUCTION

The fatigue fracture of structural details subjected to cyclic loads mostly occurs at a critical cross section with stress concentration. In a welded joint (Fig. 1), fatigue crack initiates at the weld toe and propagates through the main plate to a final fracture.

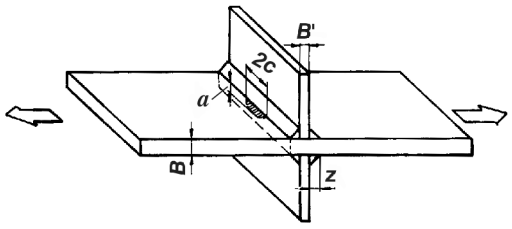

Fig.1. Welded joint

Received April 04, 2003

Since very small and sharp defects are present at the weld toe, the crack initiation phase is very short. According to this fact, the total fatigue life could be estimated by integrating the equation of the crack growth rate (e.g. Paris equation [1]) from an initial crack size a_0 (crack-like defect) to the final crack size a_f, corresponding to the final fracture of the welded joint:

$$\frac{da}{dN} = C(\Delta K)^{m} \tag{1}$$

$$N_T = \int_{a_0}^{a_f} \frac{da}{C(\Delta K)^{m}} \tag{2}$$

However, Eq. (1) underestimates the propagation rates of short cracks within a local plastic zone surrounding the notches (experimentaly determined short crack rates are significantly higher than predicted ones). Also, the crack growth rate decreases at the beginning of the short crack growth within the local plastic zone and for stress ranges below fatigue limit the crack stops becoming "non-propagating crack". This phenomenon is explained by assuming that the short crack grows through the local plastic zone under notch plasticity control. Its rate decreases because of the decreasing strains in that zone. After the end of the notch plastic zone, crack grows under a crack tip plasticity control.

These observations show that ΔK parameter is unable to describe the short crack growth within the local plastic zone surrounding the notches. Several parameters have been proposed to quantify the short crack growth rate within a notch plastic zone: strain intensity factor, cyclic *J*-integral. The growth rates of short and long cracks in a low carbon steel were uniquely caracterized by using ΔK_{eff} in Ref. [2]. Namely, Elber [3] established fatigue crack closure concept, according to which, the crack can not propagate whilst it remains closed. Consequently, ΔK is replaced by the effective SIF range in the fatigue crack growth rate equation:

$$\frac{da}{dN} = C(\Delta K_{eff})^{m} \tag{3}$$

where

$$\Delta K_{eff} = K_{max} - K_{cl}$$

or

$$\Delta K_{eff} = U_{eff}\,\Delta K \quad \text{with} \quad U_{eff} = \frac{K_{max} - K_{cl}}{K_{max} - K_{min}} \tag{4}$$

where K_{cl} is stress intensity factor corresponding to the crack closure.

Since there are no available data to enable the prediction of closure level of various geometry and loading conditions, a reasonable approximation is made according to the boundary conditions: at the nocth root the crack is fully open i.e. $U_{eff} = 1.0$, at the end of the notch plastic zone (at distance a_{pz}) the crack closure level reaches its stabilized value for a long crack i.e. $U_{eff} = U_s$. The decrease of U_{eff} within the weld toe plastic zone is described by straight lines AB and BC (Fig. 2):

$$\left.\begin{aligned} &\text{AB}: \quad U_{\text{eff}} = 1 - 2(1-U_{\text{s}})\frac{a}{a_{\text{pz}}} && \text{if} \quad a \le a_{\text{B}} \\ &\text{BC}: \quad U_{\text{eff}} = 0.5(1+U_{\text{s}}) - 0.5(1-U_{\text{s}})\frac{a}{a_{\text{pz}}} && \text{if} \quad a_{\text{B}} < a \le a_{\text{pz}} \\ &\text{CD}: \quad U_{\text{eff}} = U_{\text{s}} && \text{if} \quad a > a_{\text{pz}} \end{aligned}\right\} \tag{5}$$

where a_{pz} = size of the local plastic zone. Eqs. (5) were chosen in order to give a good agreement with a transient variation of the crack closure level obtained by numerical analyses as reported in Ref. [4,5]. The stabilized value U_{s} for a long crack is equal to 0.40 ($K_{\text{cl}}/K_{\text{max}}$ = 0.20) under $R = -1$ loading (according to Ref. [6]). Stress ratio $R = -1$ is assumed in this work because of a more pronounced short crack behavior than for zero or positive R-ratios.

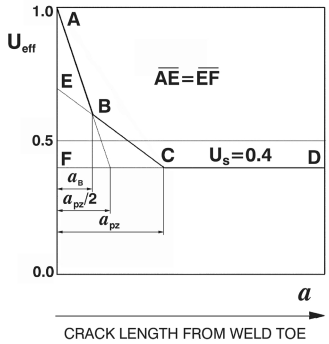

Fig. 2. Approximated crack closure level vs crack length under $R = -1$ loading

Determination of stress intensity factor

Many experimental data show that fatigue cracks in welded joints have semi-elliptical front shape. The values of $a/2c$ = 0-0.1 ($a/2c$ = 0 for straight crack front) in automatically welded joints have been reported in Ref. [7] (a = crack size, minor semi-axis of elliptical crack; c = major semi-axis of elliptical crack). In this work it was assumed the value of $a/2c$ = 0 for which K increases more quickly than for semi-elliptical cracks, so that a greater part of total fatigue life is consumed when the crack is short.

The stress intensity factor was calculated by using the expression:

$$K = \frac{M_{\text{s}} M_{\text{t}} M_{\text{k}}}{\phi_0} \sigma \sqrt{\pi a} \tag{6}$$

where M_{s}, M_{t}, ϕ_0, M_{k} are correction factors modifying the value of K of the idealized case in order to take account, respectively, of the free surface, the finite thickness, the crack front shape and a non-uniform stress distribution. The correction factors are determined (for $a/2c$ = 0) by using Gross' solution [8]:

$$\frac{M_s M_t}{\phi_0} = 1.122 - 0.231\left(\frac{a}{B}\right) + 10.55\left(\frac{a}{B}\right)^2 - 21.7\left(\frac{a}{B}\right)^3 + 33.19\left(\frac{a}{B}\right)^4 \tag{7}$$

and Albrecht's solution [9]:

$$M_k = \frac{2}{\pi}\sum_{i=1}^{n}\frac{\sigma_{bi}}{\sigma}\left(\arcsin\frac{b_{i+1}}{a} - \arcsin\frac{b_i}{a}\right) \tag{8}$$

where σ_{bi} = the normal stress in a finite element between the distance b_i and b_{i+1}; σ = the nominal stress. Verreman *et al.* [6] used this method for the determination of the stress intensity factor of a cruciform-welded joint and compared it with the accurate solution obtained by Smith [10] using high-order crack tip elements with an inverse square root singularity. They reported differences smaller than 6 %, so this method can be considered accurate for engineering purposes. The advantage of Albrecht's method is that only one stress analysis needs to be made for each joint geometry, i.e. the stress analysis of an uncracked joint.

Stress distribution along the potential crack path (in the uncracked joint) was determined by using the elasto-plastic finite element analysis [6] (Fig. 3). The geometry parameters were: the thickness $B = B' = 12.7$ mm; the weld toe radius $r = 0.05$ mm; the weld leg size $z/B = 0.5$ and the weld toe angle $\theta = 45°$.

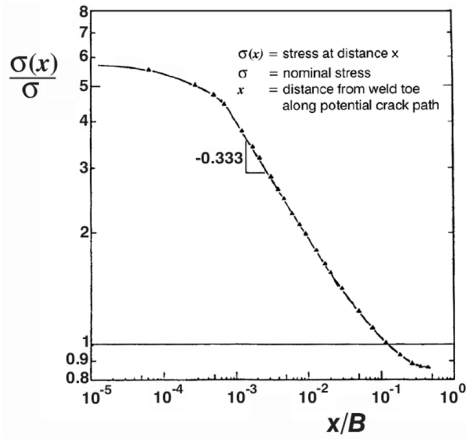

Fig. 3. Stress distribution along potential crack path in the uncracked welded joint

Except for a very small zone near the weld toe, the stress distribution is linear on log-log plot (Fig. 3) and can be expressed with only a 0.7 % error by [6]:

$$\frac{\sigma(x)}{\sigma} = \left(\frac{x}{B}\right)^{-\alpha}\sum_{i=0}^{4}\lambda_i\left(\frac{x}{B}\right)^i \tag{9}$$

The coefficients α and λ_i are given in Table 1.

Table 1. Values of α and λ_i coefficients for $\theta = 45°$

$\theta = 45°$			$\alpha = 0.333$		
i	0	1	2	3	4
λ_i	0.414	0.815	−1.71	4.16	−3.70

The size of the local plastic zone at the weld toe depends on maximum nominal stress σ_{max} (Fig.4).

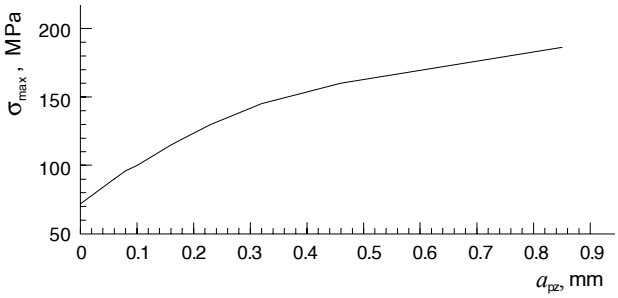

Fig. 4. Size of the local plastic zone vs maximum nominal stress

FATIGUE LIFE PREDICTION OF A WELDED JOINT

The material and geometry parameters listed below are taken from Ref. [6]. The base metal for the considered welded joint is ASTM A36 mild steel. The yield stress is σ_{ys} = 188 MPa. Material constants are $m = 4$, $C = 4.3 \cdot 10^{-10}$, while da/dN is expressed in mm/cycle and K in MPa$\sqrt{\text{m}}$. The effective threshold stress intensity range $\Delta K_{\text{eff, th}}$ = 3.9 MPa$\sqrt{\text{m}}$. The initial crack-like defect size a_0 = 0.02 mm; this value was chosen according to Smith's investigation on welded toe defects [11]. The critical final crack size a_f was chosen to correspond to $da/dN = 10^{-2}$ mm/cycle. For simplicity, the influence of the microstructural heterogeneity and residual stress was not considered in this paper.

Constant-amplitude Fatigue

Fatigue lives of the welded joints were obtained from the equation:

$$N_{\text{TCA}} = \int_{a_0}^{a_f} \frac{da}{C(\Delta K_{\text{eff}})^{\text{m}}} \tag{10}$$

The values of ΔK_{eff} were calculated from Eqs.(4-8) for the known stress distribution. The equation (10) was solved by 32-point Gaussian quadrature method. These calculations were performed by using the computer program based on this procedure. Numerical integration was performed for several values of $\Delta\sigma$ until the constant-amplitude fatigue limit is reached (minimum ΔK_{eff} during the crack growth is equal to $\Delta K_{\text{eff, th}}$). The S-N curve was determined by the regression analysis (Fig. 5).

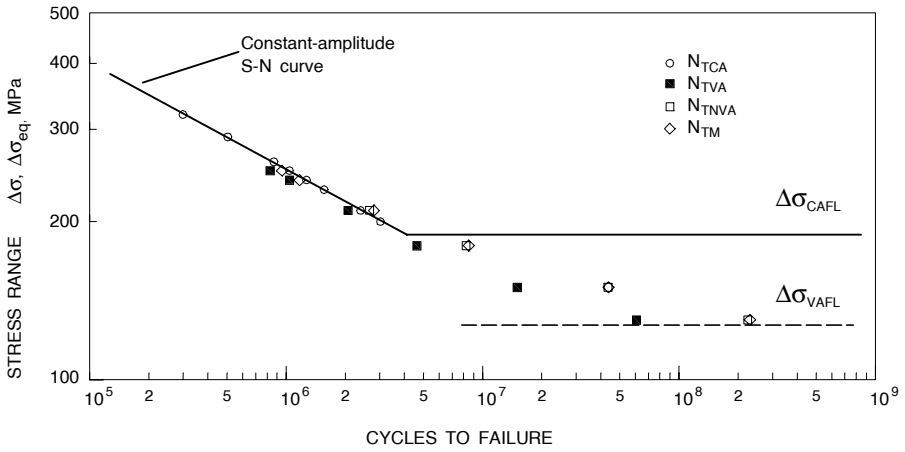

Fig. 5. Predicted fatigue lives: N_{TCA} - Constant-amplitude fatigue, N_{TVA} - Variable-amplitude fatigue, N_{TNVA} - Neglecting $\Delta\sigma_i < \Delta\sigma_{CAFL}$; N_{TM} - Miner's rule

Variable-amplitude fatigue

The welded joint was subjected to a block-spectrum loading (Fig. 6). The normalized stress ranges ($\Delta\sigma_i/\Delta\sigma_{max}$) and the frequency of each stress level (γ_i) are given in Table 2. Stress ratio is $R = -1$. The spectrum size, 1000 cycles, was chosen to avoid interactive effects (as a consequence of "delayed retardation") according to Ref. [12,13].

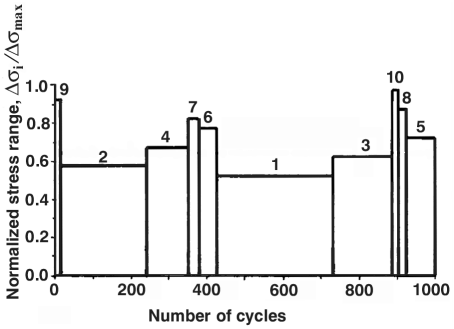

Fig. 6. Block spectrum loading pattern

Table 2. Data for block-loading spectrum

Block number *i*	1	2	3	4	5	6	7	8	9	10
Normalized stress range $\Delta\sigma_i/\Delta\sigma_{max}$	0.525	0.575	0.625	0.675	0.725	0.775	0.825	0.875	0.925	0.975
Frequency γ_i, %	30.6	22.3	15.9	10.8	7.2	4.7	3.1	2.1	1.7	1.6

Fatigue lives of the welded joint subjected to variable-amplitude loading were determined by solving Eq. (3) from a_0 to a_f using the Runge-Kutta method incorporated in the computer program designed for a simulation of fatigue crack growth [14]. The lives are plotted in Fig. 5 against the equivalent stress range $\Delta\sigma_{eq}$ of the spectrum. The equivalent stress range is given by the equation

$$\Delta\sigma_{eq} = \left[\sum_{i=1}^{n} \gamma_i (\Delta\sigma_i)^m\right]^{1/m} = \left[\sum_{i=1}^{n} \gamma_i \psi_i^m\right]^m \Delta\sigma_{max} = \rho\Delta\sigma_{max} \tag{11}$$

where $\psi_i = \Delta\sigma_i / \Delta\sigma_{max}$. These calculations were performed for several $\Delta\sigma_{eq}$, until the variable-amplitude fatigue limit is reached. The variable-amplitude fatigue limit is the value of an equivalent stress range of the spectrum with the maximum stress range $\Delta\sigma_{10}$ which is equal to the constant-amplitude fatigue limit i.e. whose minimum ΔK_{eff} during crack growth reached $\Delta K_{eff,\,th}$ value. The calculated fatigue lives N_{TVA} are given in Table 3.

Table 3. Predicted lives for variable-amplitude fatigue

1	2	3	4	5	6
Equivalent stress range $\Delta\sigma_{eq}$ (MPa)	Predicted fatigue life N_{TVA} (kilocycles)	Miner's rule N_{TM} (kilocycles)	Predicted life neglecting $\Delta\sigma_i < \Delta\sigma_{CAFL}$ N_{TNVA} (kilocycles)	Ratio N_{TVA}/N_{TM}	Ratio N_{TNVA}/N_{TM}
250	827	953	827	0.87	0.87
240	1035	1165	1035	0.89	0.89
210	2055	2822	2660	0.73	0.94
180	4619	8495	8224	0.54	0.97
150	14968	43792	43650	0.34	1.00
130	60551	229711	223550	0.26	0.97

Fatigue lives of the welded joint were also calculated by using Miner's cumulative damage rule [15]:

$$\sum_{i=1}^{k} \frac{n_i}{N_i} = 1 \tag{12}$$

where n_i = number of cycles at the range $\Delta\sigma_i$ in the total fatigue life, and N_i = number of cycles at constant stress range $\Delta\sigma_i$ that produces the failure. From the Eq. (12) and equation of the S-N curve, the total fatigue life can be expressed as

$$N_{TM} = \frac{N_{10}}{\sum_{i=1}^{k} \gamma_i \left(\frac{\Delta\sigma_i}{\Delta\sigma_{10}}\right)^n} \tag{13}$$

where N_{10} = number of cycles until failure at the highest stress range $\Delta\sigma_{10}$ in the spectrum; n = the exponent of the constant-amplitude S-N curve. Damaging effects of the stress

ranges below the constant-amplitude fatigue limit are neglected according to this rule. The values of N_{TM} for the various levels of $\Delta\sigma_{eq}$ are shown in Table 3. A comparison of the total fatigue lives obtained by the computer simulation and Miner's rule (column 5) shows a good agreement for the spectra with all the stress ranges above the constant-amplitude fatigue limit ($\Delta\sigma_{eq}$ =240 and 250 MPa). The great difference is noticed for the spectra having some of the stress ranges below the constant-amplitude fatigue limit ($\Delta\sigma_{CAFL}$), especially for $\Delta\sigma_{eq}$ near the variable-amplitude fatigue limit. This difference could be attributed to the fact that Miner's rule neglects the damaging effect of stresses below the constant-amplitude fatigue limit. However, according to the computer simulation, once a crack has started propagation under the highest stress in the spectrum, some of the low stresses which were previously non-damaging may become damaging during a crack growth (even if ΔK is still below ΔK_{th}, see Ref. [16]), so that ignoring them would be unsafe. In order to check this statement, the total fatigue lives N_{TNVA} were calculated using the computer simulation, reducing all the stress ranges lying below the constant-amplitude fatigue limit so that the corresponding ΔK_{eff} values remain less than $\Delta K_{eff,\ th}$ during the crack growth from a_0 to a_f. These fatigue lives N_{TNVA} show a good agreement with Miner's solution for all $\Delta\sigma_{eq}$ levels (Table 3., column 6). Hence it may be concluded: if the computer simulation with artificial elimination of the damaging effect of stress ranges below the constant-amplitude fatigue limit gives the results (N_{TNVA}) close to Miner's rule (N_{TM}), then this computer simulation accounting for the damaging effect of all stress ranges in the spectrum can be considered as a sufficiently accurate method. The computer simulation quantified an overestimation of the total fatigue lives obtained by Miner's rule: e. g. for the spectrum with $\Delta\sigma_{eq}$ = 130 MPa (near the variable-amplitude fatigue limit) computer simulation gives the fatigue life which is 26% of the corresponding fatigue life obtained by Miner's rule.

The computer simulations were performed on Pentium 2 by using Compaq Visual Fortran that enables a very high speed of the simulation.

CONCLUSIONS

A structural detail subjected to variable-amplitude loading is considered in this work. The computer simulation of the fatigue crack growth was performed in that purpose. The computer program, designed for this simulation, takes into account the material properties, detail geometry, loading conditions, short and long crack behaviour. An advantage of this simulation is that it enables a prediction of the fatigue life in the region where Miner's rule gives great errors. Further development of this program could take into account an influence of residual stress, microstructure and interactive effects.

REFERENCES

1. P. C. Paris (1965) The fracture mechanics approach to fatigue, In Proceedings of the Tenth Sagamore Conference, Syracuse University Press, New York, p.107
2. K. Tanaka and Y. Nakai (1983) Propagation and non-propagation of short fatigue cracks at a sharp notch, Fatigue Engng Mater. Struct., Vol.6, pp.315-327
3. W. Elber (1971) The significance of fatigue crack closure, ASTM STP 486, pp.230-242

4. K. Ohji *et al.* (1975) Cyclic analysis of a propagating crack and its correlation with fatigue crack growth, Engng Fract. Mech., Vol.7., pp.457-464
5. J.C.Jr. Newman (1981) A crack closure model for predicting fatigue crack growth under aircraft spectrum loading, ASTM STP 748, pp. 53-84
6. Y. Verreman, J.P. Bailon and J. Masounave (1987) Fatigue life prediction of welded joints–a re-assessment, Fatigue Fract. Engng Mater. Struct., Vol.10, pp.17-36
7. A. Sahli and P. Albrecht (1984) Fatigue life of welded stiffeners with known initial cracks, In Fracture Mechanics, Proceedings of Fifteenth Symposium, ASTM STP 833, pp. 193-217
8. B. Gross *et al.* (1964) Stress intensity factors for a single-edge-notch tension specimen by boundary collocation of a stress function, NASA Tech. Note D-2395
9. P. Albrecht and K. Yamada (1977) Rapid calculation of stress intensity factors, J. Struct. Division, ASCE, Vol.103, pp. 377-389
10. I.J. Smith (1984) The effect of geometry changes upon the predicted fatigue strength of welded joints, In Proceedings of the Third International Conference on Numerical Methods in Fracture Mechanics, Pineridge Press, Swansea, UK, pp. 561-574
11. I.F.C. Smith and R.A. Smith (1982) Defects and crack shape development in fillet welded joints, Fatigue Engng Mater. Struct., Vol.5, pp. 151-165
12. A. Abtahi, P. Albrecht and G.R. Irwin (1977) Fatigue strength of a structural detail subjected to single and periodic overloads, In Mechanics in Engineering, University of Waterloo Press, pp. 313-334
13. E.F.J. Von Euw, R.W. Hertzberg and R. Roberts (1972) Delay effects in fatigue crack propagation, ASTM STP 513, pp. 230-259
14. Z. Perovic (1998) Bimodal concept of high-cycle fatigue life prediction for constant and variable amplitude fatigue, Fatigue Fract. Engng Mater. Struct., Vol. 21, 1559-1574
15. M.A. Miner (1945) Cumulative damage in fatigue, J. Appl. Mech. Vol. 12, Trans. ASME, Vol. 67, A-159-164
16. K.J. Miller (1997) The three thresholds for fatigue crack propagation, ASTM STP 1296, pp. 267-286

KOMPJUTERSKA SIMULACIJA AKUMULACIJE ZAMORNOG OŠTEĆENJA

Zoran Perović

U ovom radu je prikazana kompjuterska simulacija akumulacije zamornog oštećenja u zavarenom spoju izloženom opterećenju sa promjenljivom amplitudom. Brzina rasta zamorne prsline za dati materijal je izražena kao funkcija od ΔK_{eff} u cilju obuhvatanja ponašanja i kratke i duge prsline. Korekcioni faktori u izrazu za K-faktor su određeni kombinacijom Gross-ove i Albrecht-ove metode. Zamorni vijek je izračunat rješavanjem jednačine brzine rasta zamorne prsline od a_0 do a_f pomoću metode Runge-Kutta. Kompjuterski program, baziran na ovoj proceduri, korišćen je za simulaciju rasta zamorne prsline. Dobijeni rezultati su upoređeni sa zamornim vijekom određenim pomoću Miner-ovog pravila. Na ovaj način je određena greška Miner-ovog pravila za područje u blizini zamorne čvrstoće za promjenljivu amplitudu.